

# Biomaterial-induced sarcomagenesis is not associated with microsatellite instability

Achim Weber · Annette Strehl · Erik Springer ·  
Torsten Hansen · Arno Schad · C. James Kirkpatrick

Received: 18 June 2008 / Revised: 4 October 2008 / Accepted: 13 November 2008 / Published online: 19 December 2008  
© Springer-Verlag 2008

**Abstract** Sarcomagenesis, in contrast to carcinogenesis, is poorly understood. Microsatellite instability has been implicated in the development of many cancers, in particular those associated with chronic inflammatory conditions. In an experimental animal model, rats developed not only a peri-implantational chronic inflammatory reaction, but also malignant mesenchymal tumors in response to different biomaterials. Therefore, it was the aim of our study to test if the development of biomaterial-induced sarcomas is characterized by a mutator phenotype. A multiplex-PCR approach was designed to screen biomaterial-induced sarcomas for the presence of microsatellite instability. Seven different microsatellite loci were tested in ten tumors for microsatellite instability using a fluorochrome-labelled multiplex-PCR and subsequent fragment analysis. All tumors provided a microsatellite-stable phenotype at all loci tested. Our data suggest that microsatellite instability is rarely or not at all a feature of malignant transformation of biomaterial-induced soft tissue tumors. Thus, there is no evidence that a mutator phenotype is a hallmark of biomaterial-induced sarcomagenesis.

**Keywords** Biomaterials · Sarcoma · Microsatellite instability · Mutator phenotype

## Introduction

Tumorigenesis is now widely accepted as resulting from a stepwise accumulation of genetic instability [1]. The biological and molecular mechanisms involved in the development of carcinomas in humans and mammals have been extensively investigated. In contrast, the molecular steps in the development of sarcomas and other soft tissue tumors are less well understood. A progression from a benign precursor lesion to malignant tumor, characteristic of many epithelial tumors, is exceptional for soft tissue tumors. However, a biological continuum of benign and malignant soft tissue tumors has been postulated for example in the case of lipomatous [2] and nerve sheath tumors [3, 4].

In a previous study, we had established an animal model for the tumorigenesis of soft tissue tumors [5]. Malignant mesenchymal tumors were induced around subcutaneously implanted biomaterial disks. In addition to fully developed tumors, implantation sites showed lymphocyte and macrophage infiltrates reflecting an inflammatory reaction, as a characteristic response to the implantation of foreign materials [6, 7] as well as hyper-proliferative lesions, reflecting precursor lesions. This animal model allowed a detailed investigation of sarcoma tumorigenesis, especially because a spectrum of preneoplastic lesions could be identified.

Several mechanisms are known to result in genetic instability and consequent malignant transformation of cells. One pathway is the development of chromosomal instability with numerical and structural chromosomal

---

A. Weber · A. Strehl · E. Springer · T. Hansen · A. Schad ·  
C. J. Kirkpatrick  
Institute of Pathology, Johannes Gutenberg University of Mainz,  
Langenbeckstr. 1,  
55101 Mainz, Germany

### Present address:

A. Weber (✉)  
Department of Pathology, Institute of Surgical Pathology,  
University Hospital of Zurich,  
Schmelzbergstr. 12,  
8091 Zurich, Switzerland  
e-mail: achim.weber@usz.ch

changes and aneuploidy of tumor cells. Another pathway is the development of a “mutator phenotype” with changes at the nucleotide level. These alterations may result in the accumulation of multiple mutations in genes relevant to cell growth and homeostasis, eventually leading to growth advantage and transformation of cells. Multiple short tandem repetitive DNA-sequences, also known as microsatellites, are present throughout the genome of humans and other mammals [8]. A mutator phenotype is frequently reflected by widespread sequence length alterations of these microsatellites, designated as microsatellite instability [9, 10]. Besides inherited deficiencies of mismatch repair (MMR) genes and inactivation by methylation, an underlying impairment of repair enzymes in association with chronic inflammation [11, 12] has been demonstrated, most likely due to oxidative stress [13].

While there is a clear association of specific or typical chromosomal translocations or translocation of gene fusion products with many soft tissue tumors, microsatellite instability has also been reported for some entities [14–17]. Since a chronic inflammatory condition is associated with microsatellite-associated carcinogenesis, we sought to investigate if the tumorigenesis of biomaterial-induced sarcomas is based on the development of a mutator phenotype. Using the above-mentioned rat model, biomaterial-induced sarcomas were screened for microsatellite instability.

## Materials and methods

### Animal model

Ten formalin-fixed, paraffin-embedded tumor samples (Table 1) were retrieved from the previously published rat sarcoma collective [5]. Briefly, in this study a total of 490 Fischer rats had been implanted with nine different standard medical grade biomaterials. In about one quarter of implantations, animals developed (mostly malignant) mesenchymal tumors of different histological type, including fibrosarcomas,

leiomyosarcomas, and rhabdomyosarcomas, around the implantation sites.

### Laser capture microdissection

Sections of normal and transformed tissues (either tumors or precursor lesions) from the above mentioned paraffin blocks were prepared on membrane mounted-slides (PALM MembraneSlides, P.A.L.M., Bernried, Germany) and de-paraffinized. Microdissection was performed using a PALM MicroBeam system with a pulsed UV-A nitrogen laser (337 nm). The selected areas were marked, cut out, and pulsed into a 0.5-ml microfuge tube with adhesive filling (PALM AdhesiveCaps, P.A.L.M.), taking care to keep the normal and tumor tissues separate. “Normal tissue” was prepared so distant from the implantation site that it was morphologically not affected by the implants and corresponding tissue reactions.

### Multiplex PCR and fragment analysis

Since (in contrast to human and mouse) no well-established and characterized panels of markers for the analysis of microsatellite instability was described in rat, sequence information of rat microsatellite loci was taken from several studies [18–20]. In order to compensate for a potentially low sensitivity of these markers in detecting MSI, seven markers instead of the more common panel of five markers was used (Table 2). DNA was isolated by proteinase K digestion, followed by phenol-chloroform extraction and ethanol/salt precipitation using standard protocols [21]. Two multiplex PCR-reactions were performed using two different primer mixtures with fluorochrome-labelled oligonucleotide primers. In each case, either the forward or the reverse primer was fluorochrome-labelled. Primermix A contained oligonucleotide primers of the loci GH, NGFR, SECR, and UCP; primermix B contained oligonucleotide primers of the loci ANF, PPY, and SMST (Table 2). Non-fluorescent oligonucleotide primers were purchased from

**Table 1** Biomaterial-induced soft tissue tumors

	Code	Implanted biomaterial	Tumor
	46 PU 101	Aliphatic polyurethane	Pleomorphic rhabdomyosarcoma
	11 PMMA 84	Polymethylmethacrylate	Osteosarcoma
	1 PMMA 86	Polymethylmethacrylate	Sarcoma, NOS
	16 Si 80	Silicone	Pre-neoplastic lesion
	2 Si 90	Silicone	Sarcoma, NOS
	4 PVC 105	Polyvinyl chloride	Fibrosarcoma
	5 NiCr 107	Nickel chromium	Dedifferentiated liposarcoma
	25 NiCr 107	Nickel chromium	Pleomorphic sarcoma
	24 Alu 103	Aluminum	Spindle cell sarcoma
	1 Si 87	Silicone	Sarcoma, NOS

The study included a total of ten different biomaterial-induced soft tissue tumors. Every rat was given an identification code describing the implanted material. The resulting tumor was histologically diagnosed

**Table 2** Microsatellite loci and oligonucleotide primer sets

Locus	Acc. No.	Oligo nucleotide sequence	Size <sup>a</sup>	Dye	Ref.
Mix A					
GH	X12967	F 5'-ATGGGAGGGAACAAGTCTTC-3' R 5'-GAGGGAGAGAGAAAGAGAGACAG-3'	135	D4	[18, 19]
NGFR	X05137	F 5'-ACCCACAATCCAACACTATAC-3' R 5'-GCAGGATCTAGTCTCAGCCC-3'	126	D3	[18, 19]
SECR	M64033	F 5'-ACCATGGAGCCTCTACTGC-3' R 5'-GTCCCGTCCGAGTGTCTT-3'	194	D4	[18, 20]
UCP	X12925	F 5'-TGCCCGTCTCTGTTACTCAT-3' R 5'-CAAGAACCCTGAGGCAATAA-3'	111	D4	[18, 19]
Mix B					
SMST	K02248	F 5'-TTTCCAGGTGCCAAATGTAG-3' R 5'-TATATTGTGACAAAAGAAAGGCAC-3'	154	D4	[18, 20]
ANF	K02062	F 5'-TCCACAACCTTGATCTTTTCG-3' R 5'-GTTGAGGGCCATAGTGTGAC-3'	160	D2	[18, 20]
PPY	M27450	F 5'-CACACTGACCAGGCCTAGG-3' R 5'-TGTCAGCTCAGCTGCTTTG-3'	153	D3	[18, 20]

Microsatellite loci and oligonucleotide primer sequences information

*GH* growth hormone, *NGFR* nerve growth factor receptor, *SECR* secretin, *UCP* uncoupling protein, *SMST* somatostatin, *ANF* atrial natriuretic factor, *PPY* pancreatic polypeptide

<sup>a</sup> Sizes are indicated as expected according to NCBI database information and differed significantly from the fragment sizes observed in this study in case of the GH, UCP, and PPY loci, respectively

biomers.net, Ulm, Germany and the fluorescent oligonucleotide primers from Sigma-Aldrich, Germany.

The final 25- $\mu$ l multiplex reaction mix consisted of the following: 12.5  $\mu$ l Qiagen-Multiplex-Mastermix (Qiagen, Hilden, Germany), 2.5  $\mu$ l 10 $\times$  primer-mix, 7.5  $\mu$ l H<sub>2</sub>O, and 2.5  $\mu$ l template. The 10 $\times$  primer-mix was composed by mixing 50  $\mu$ M fluorescent primers and 100  $\mu$ M non-fluorescent primers at a concentration of 2  $\mu$ M each in H<sub>2</sub>O.

PCR was performed using a GeneAmp 9700 thermocycler (Applied Biosystems, Foster City, CA, USA) under the following conditions: initial denaturation at 95 $^{\circ}$  for 15 min, followed by 45 cycles of: 30 s at 94 $^{\circ}$ , 90 s at 54 $^{\circ}$ , and 1 min at 72 $^{\circ}$  with a final 30-min extension period at 60 $^{\circ}$ . The resulting PCR-product was then analyzed by gel-electrophoresis on a 2% agarose gel and subsequent fragment analysis of the fluorescently labelled PCR products was performed using a Beckman Coulter CEQ 8000 Sequencer (Beckman Coulter, Krefeld, Germany) with the corresponding CEQ System software. The detected fragments of normal and malignant tissue were compared to determine the stability for each locus.

## Results

### Tissue selection and isolation of tumor and normal DNA

Histology of the samples was re-evaluated in order to define suitable areas of tumor and non-neoplastic tissue, respectively. In all cases studied, a clear identification of

tumors and non-tumorous areas was possible, providing the basis for the laser-capture analysis and tissue preparation (Fig. 1). Following laser-capture (P.A.L.M.)-based tissue preparation and standard nucleic acid extraction, a sufficient amount and quality of DNA could be isolated from all samples analyzed.

### Development of a multiplex-PCR assay for microsatellite instability testing

PCR conditions were first optimized, and all samples were initially tested in a single PCR setting. In the case of the GH and PPY locus, respectively, significantly lower amplification sizes were observed when compared to information from either the gene bank (see Table 2) and/or the literature [18]. In the case of the PPY locus, higher amplification sizes were observed. The SECR locus revealed rather a single peak instead of the characteristic stuttering pattern in all samples tested. However, all loci displayed a constant size comparing different animals (due to the same genetic background of animals).

After successfully testing each pair of oligonucleotide primers in a single-PCR, a multiplex-PCR-assay was designed by dividing the seven different primers into two groups of three or four primer pairs, respectively. Using this multiplex-PCR approach, all loci test were successfully amplified and analyzed by fluorescence-based fragment analysis. No difference between single PCR fragment analysis patterns and the multiplex approach was observed,

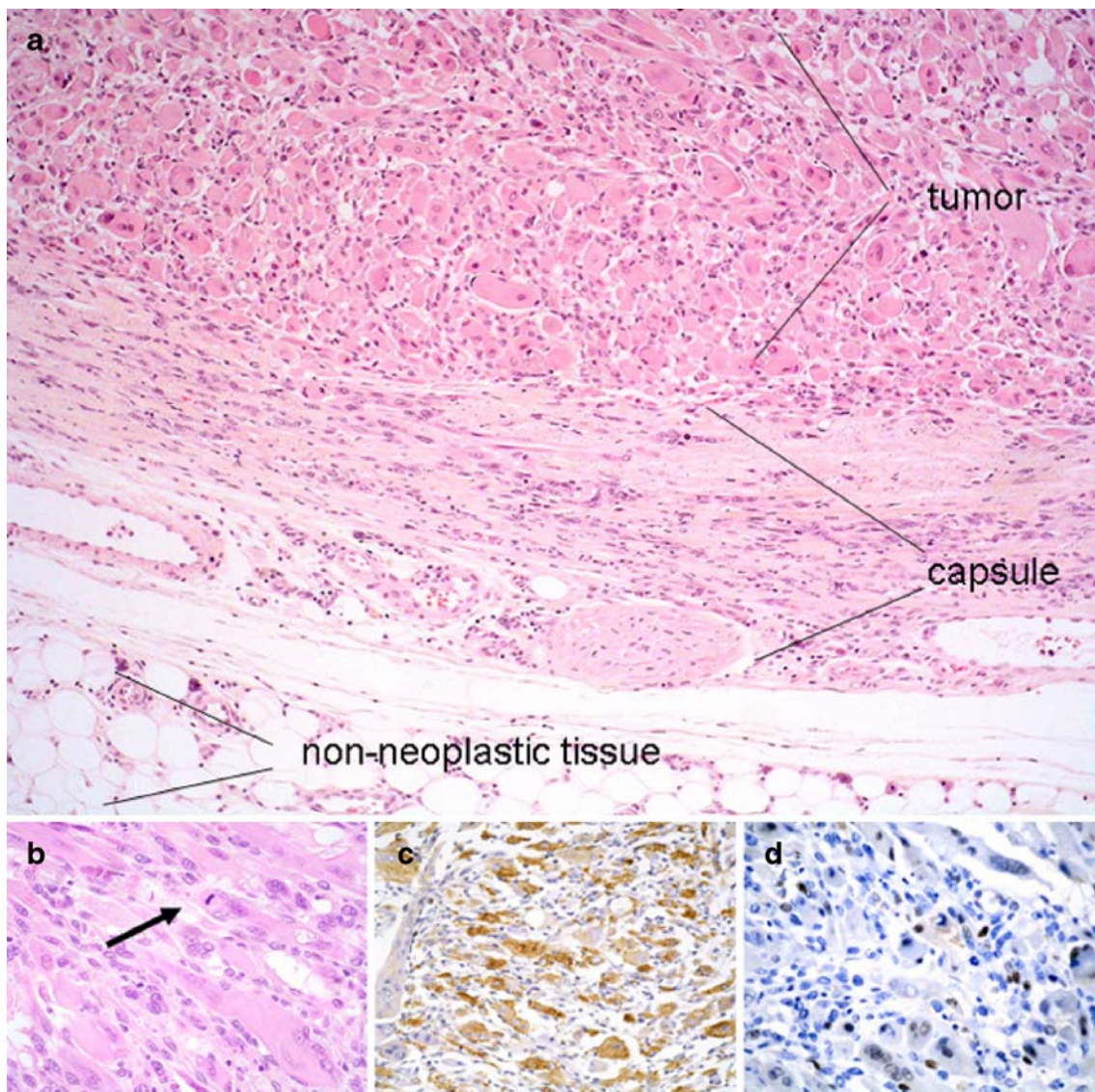


**Fig. 1** Examples of a biomaterial-induced sarcoma (pleomorphic rhabdomyosarcoma from animal 46 PU 101). **a** Histology revealed a pleomorphic tumor with rhabdomyoblastic differentiation (*upper left*) and a rather well-defined border surrounded by a fibrous connective tissue capsule with proliferative lesions, possibly pre-neoplastic. (Tissue for DNA isolation was prepared by laser-microdissection

from tumors, capsule tissue, and surrounding non-neoplastic tissue, respectively). **b** Higher magnification of the tumor shows atypical tumor cells with vacuoles similar to lipoblasts and a mitotic figure (*arrow*). **c** Tumor cells show a widespread positive cytoplasmic immunoreactivity for desmin, **d** as well as a strong nuclear positivity for myogenin

indicating that the multiplex assay used was a valid method for the simultaneous testing of several microsatellite loci (Fig. 2).

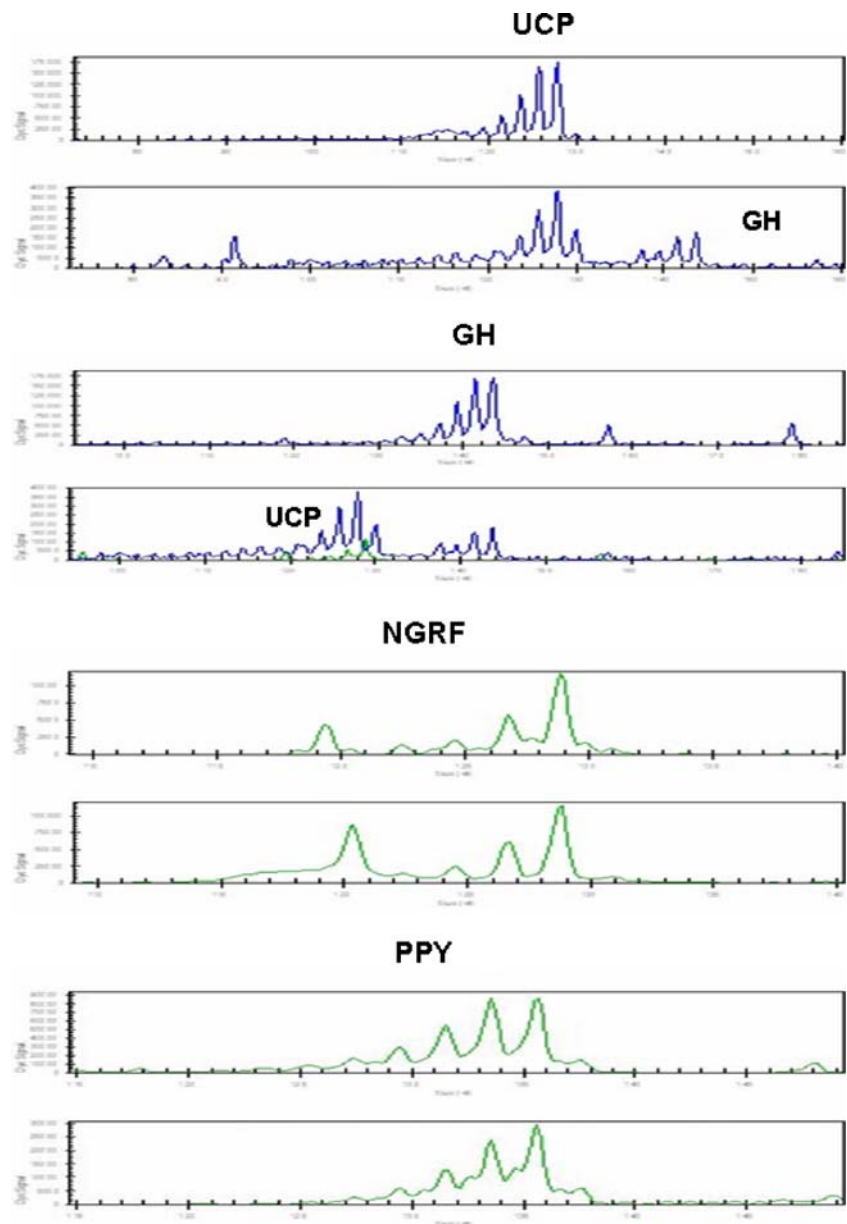
All microsatellite loci showed a stable phenotype

A total of 140 microsatellites was analyzed, with 70 microsatellites displaying microsatellites of neoplastic or preneoplastic tissue, and the other 70 reflecting the corresponding normal tissue, respectively. Nearly all microsatellites were informative with the exception of three cases (PND locus of animals: one PMMA 86, two Si90, and four

PVC 105). In these cases, the fragment analysis revealed signals which were too low or unspecific to be readable, so that a definite statement about the stability of the microsatellite loci for these particular samples could not be made.

For all other microsatellite loci tested, no size or frame shifts were observed on comparing normal and the tumor/precursor lesion tissue (see examples in Fig. 3). Thus, even assuming that the PND locus in case of the three tumors, in which this particular locus was not amplified, had shown a change in microsatellite pattern, the overall diagnostic criteria for microsatellite instability would not have been fulfilled. Therefore, all loci provided stable microsatellites.

**Fig. 2** Comparison of microsatellite profiles in single versus multiplex amplification show no changes in microsatellite patterns. In each pair, the microsatellite pattern from the single PCR amplification is shown in the *upper row* and the profile of the multiplex amplification is shown in the *lower row*. (In case of NGRF and PPY, respectively, only one locus is shown while the fluorochromes of further loci are not displayed). Amplificates result from tumor DNA of animal 5 NiCr 107 showing loci UCP and GH and NGFR loci (primer mix A) and locus PPY (primer mix B)



## Discussion

The etiology of most benign and malignant soft tissue tumors is unknown. The vast majority of soft tissue tumors seem to arise without an apparent causative factor. Among suspected or proven causative factors are genetic and environmental factors, viral infections, immune deficiencies, local environmental factors like scars or implants as well as chronic inflammatory conditions. In contrast to many epithelial tumors, a clear multistage tumorigenesis or a clear precursor-sarcoma-sequence so far has rarely been identified in soft tissue tumors. However, the demonstration of common genetic alterations in the case of benign and malignant lipomatous tumors [2, 22] as well as benign and

malignant nerve sheath tumors [3, 4] makes it reasonable that a stepwise development in soft tissues tumors is relevant for at least some entities.

In a previous study, an experimental animal model has been presented in which a high incidence of malignant soft tissue tumors arose around implanted biomaterials [5]. Sarcoma induction by biomaterials required direct contact with the respective substances. Remarkably, a broad spectrum of soft tissue tumors developed, obviously independent of the specific kind of agent implanted and lacking any consistent correlation between biomaterial groups and specific histological type of tumor. This observation suggested that it is not a specific genetic damage, interfering with a defined pathway, which is

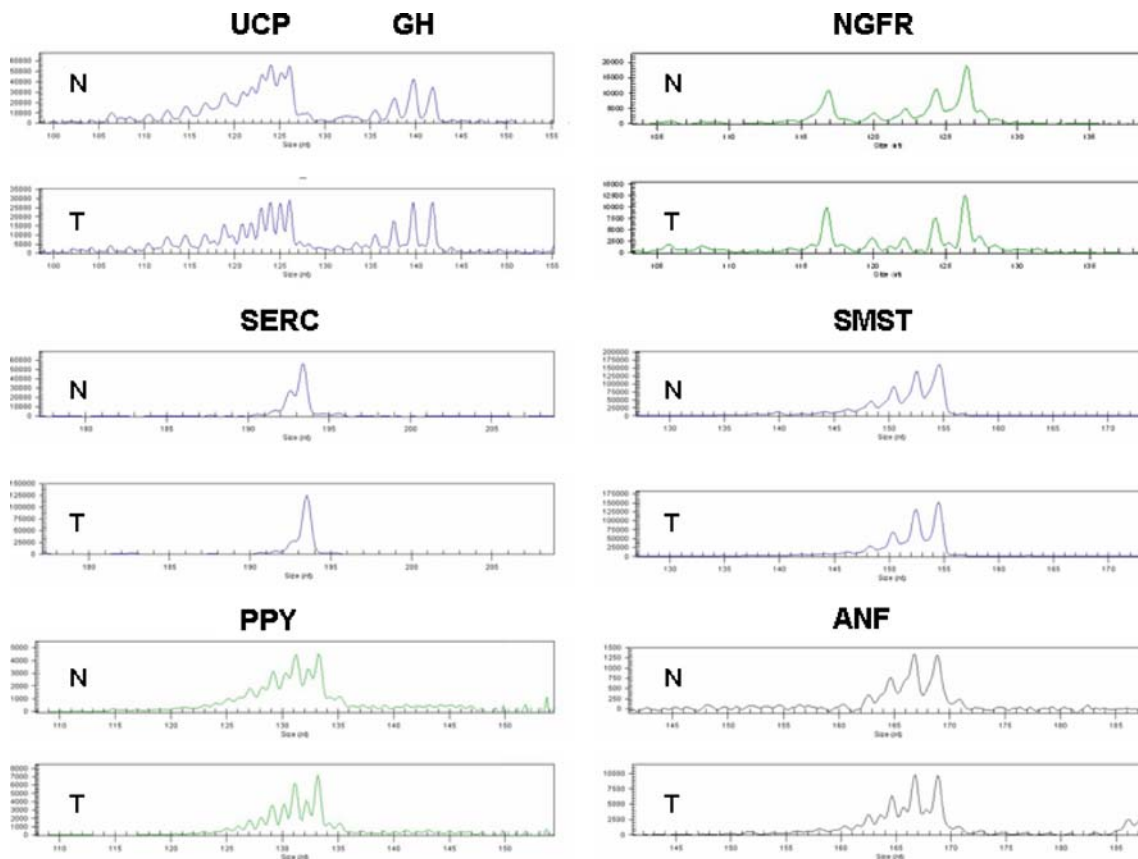


**Fig. 3** No difference in microsatellite profiles comparing tumor and normal tissue in all tumor and all seven loci tested. In each pair, the microsatellite pattern from the normal tissue (*N*) is shown in the *upper*

*row* and the pattern of the tumor (*T*) is shown in the *lower* row. Loci UCP, GH, NGFR, SERC, and PPY are shown from animal 11 PMMA 84, loci SMST, and ANF from animal 25 NiCr 107

induced. In this case, one would expect a less heterogeneous spectrum of histologic entities, as are described for several specific carcinogenic substances resulting in defined tumor entities, e.g. mesotheliomas following asbestos exposure [23]. The heterogeneous spectrum of lesions observed in this study rather argues for a (or several) more or less random insult(s). What might be the nature of this insult?

A characteristic hallmark of tumors developing in this model was the reaction of the peri-tumorous tissue, characterized by a chronic inflammation and hyperproliferative changes at peri-implantational sites, known as a typical response to foreign materials for a long time [6]. Chronic inflammation, characterized by free radical stress, can be a significant contributor to carcinogenesis [13, 24]. One could easily imagine that the microenvironment around the implants, probably through inflammation-mediated factors, might interfere with replication repair enzymes in this proliferation. Such a defect is expected to be reflected by microsatellite instability. There are several observations providing evidence that chronic inflammation indeed can result in an impaired mismatch-repair capacity, even in the absence of any genetic inactivation of the mismatch repair system [11–13]. Although rare, micro-

satellite instability has been observed in sarcomas of different histogenetic type [14, 16]. This prompted us to search for microsatellite instability in biomaterial-induced sarcomas. However, in the present study we have not observed a single microsatellite instability, neither in fully developed tumors nor in preneoplastic lesions. Based on this observation, we found no evidence that a replication-repair-associated defect is crucial for biomaterial-induced sarcomagenesis.

If this is not the case, what could be the responsible factor? As stated above, with respect to the heterogeneous spectrum of tumor entities, it seems unlikely that a specific genetic insult underlies biomaterial-induced sarcomagenesis. Although the diversity of different physical compounds able to induce soft tissue tumors argues against a direct toxic effect of substances released, there is obviously the possibility of a genotoxic effect with subsequent genetic or epigenetic changes. Alternatively, sarcomagenesis is probably associated with genetic instability on the chromosomal (cytogenetic) level, for example induced by interference with cell check points. Carcinogen-induced sarcomagenesis in Trp53+/- mice suggests that loss of p53 function is, at least in part, an important mechanism in the development of

sarcomas at the implantation site [24, 25]. Since the hypothesis that a mutator phenotype could be responsible for the development of biomaterial-induced sarcomas is not supported by our data, further investigation should test the latter possibilities.

**Acknowledgments** We thank Mrs U. Hildebrand for her expert technical assistance and the state of Rhineland-Palatinate for financial support.

**Conflict of interest** The authors declare that they have no conflict of interest.

## References

- Hanahan D, Weinberg RA (2000) The hallmarks of cancer. *Cell* 100(1):57–70
- DeiTos A, Doglioni C, Piccinin S et al (2000) Coordinated expression and amplification of the MDM2, CDK4, and HMGI-C genes in atypical lipomatous tumours. *J Pathol* 190(5):523–525
- Woodruff JM, Selig AM, Crowley K et al (1994) Schwannoma (neurilemoma) with malignant transformation. A rare, distinctive peripheral nerve tumor. *Am J Surg Pathol* 18(9):882–895
- Kindblom L, Ahlden M, Meis-Kindblom J et al (1995) Immunohistochemical and molecular analysis of p53, MDM2, proliferating cell nuclear antigen and Ki67 in benign and malignant peripheral nerve sheath tumours. *Virchows Arch* 427:19–26
- Kirkpatrick CJ, Alves A, Kohler H et al (2000) Biomaterial-induced sarcoma: a novel model to study preneoplastic change. *Am J Pathol* 156(4):1455–1467
- Brand KG, Buoen LC, Johnson KH et al (1975) Etiological factors, stages, and the role of the foreign body in foreign body tumorigenesis: a review. *Cancer Res* 35(2):279–286
- Donaldson K, Tran CL (2002) Inflammation caused by particles and fibers. *Inhal Toxicol* 14(1):5–27
- Ellegren H (2004) Microsatellites: simple sequences with complex evolution. *Nat Rev Genet* 5(6):435–445
- Ionov Y, Peinado MA, Malkhosyan S et al (1993) Ubiquitous somatic mutations in simple repeated sequences reveal a new mechanism for colonic carcinogenesis. *Nature* 363(6429):558–561
- Thibodeau SN, Bren G, Schaid D (1993) Microsatellite instability in cancer of the proximal colon. *Science* 260(5109):816–819
- Hofseth LJ, Khan MA, Ambrose M et al (2003) The adaptive imbalance in base excision-repair enzymes generates microsatellite instability in chronic inflammation. *J Clin Invest* 112(12):1887–1894
- Lee SH, Chang DK, Goel A et al (2003) Microsatellite instability and suppressed DNA repair enzyme expression in rheumatoid arthritis. *J Immunol* 170(4):2214–2220
- Chang CL, Marra G, Chauhan DP et al (2002) Oxidative stress inactivates the human DNA mismatch repair system. *Am J Physiol Cell Physiol* 283(1):C148–C154
- Ottini L, Esposito DL, Richetta A et al (1995) Alterations of microsatellites in neurofibromas of von Recklinghausen's disease. *Cancer Res* 55(23):5677–5680
- Martin SS, Hurt WG, Hedges LK et al (1998) Microsatellite instability in sarcomas. *Ann Surg Oncol* 5(4):356–360
- Sourvinos G, Parissis J, Sotsiou F et al (1999) Detection of microsatellite instability in sporadic cardiac myxomas. *Cardiovasc Res* 42(3):728–732
- Kawaguchi K, Oda Y, Takahira T et al (2005) Microsatellite instability and hMLH1 and hMSH2 expression analysis in soft tissue sarcomas. *Oncol Rep* 13(2):241–246
- Serikawa T, Kuramoto T, Hilbert P et al (1992) Rat gene mapping using PCR-analyzed microsatellites. *Genetics* 131(3):701–721
- Mironov NM, Aguelon AM, Hollams E et al (1995) Microsatellite alterations in human and rat esophageal tumors at selective loci. *Mol Carcinog* 13(1):1–5
- Walchle C, Diwan BA, Shiao YH et al (1999) Microsatellite instability is infrequent in azoxymethane-induced rat intestinal tumors: an assessment by capillary electrophoresis. *Toxicol Appl Pharmacol* 157(1):9–15
- Sambrook J, Fritsch E, Maniatis T (1989) *Molecular cloning: a laboratory manual*. Cold Spring Harbor, New York
- Mentzel T (2000) Biological continuum of benign, atypical, and malignant mesenchymal neoplasms—does it exist? *J Pathol* 190(5):531–536
- Spirtas R, Heineman EF, Bernstein L et al (1994) Malignant mesothelioma: attributable risk of asbestos exposure. *Occup Environ Med* 51(12):804–811
- Tazawa H, Tatemichi M, Sawa T et al (2007) Oxidative and nitrate stress caused by subcutaneous implantation of a foreign body accelerates sarcoma development in Trp53<sup>+/-</sup> mice. *Carcinogenesis* 28(1):191–198
- French JE, Lacks GD, Trempus C et al (2001) Loss of heterozygosity frequency at the Trp53 locus in p53-deficient (+/-) mouse tumors is carcinogen- and tissue-dependent. *Carcinogenesis* 22(1):99–106